JOURNAL OF APPLIED POLYMER SCIENCE VOL. 17, PP. 3439-3456 (1973)

Flow Properties of Aqueous Solution of Methylcellulose

TAKESHI AMARI and MATAO NAKAMURA, *Institute of Industrial Science, University of Tokyo, Roppongi, Minato-ku, Tokyo, Japan*

Synopsis

Flow properties of aqueous solution of methylcellulose, especially nonlinear viscoelasticity, were investigated. The peculiar flow properties of the aqueous solution of methylcellulose were compared with the existing theories of non-Newtonian viscosity of concentrated polymer solutions and the experimental results obtained for the aqueous solution of sodium alginate which behaves as polyelectrolyte in solution. The characteristic time for the formation of entanglement couplings between molecular chains was mainly examined. To investigate the elastic behavior under steady-shear flow, normal stress difference was measured with a coaxial cylinder apparatus, and extinction angles were determined with a flow birefringence apparatus. The values of normal stress difference obtained by the mechanical and the optical methods coincided with each other. For the aqueous solution of methylcellulose as reported for solutions of nonpolar polymers, the relation between normal stress difference and shear stress was represented by a single curve irrespective of temperature and concentration. Non-Hookean behavior was observed for the relation between recoverable shear and shear stress and attributed to the strong intermolecular interactions and the stretching-out effect of structural networks.

INTRODUCTION

It is well known that an aqueous solution of methylcellulose shows remarkable non-Newtonian viscosity and normal stress effect even in concentrations as low as a few per cent. Furthermore, peculiar temperature dependence of viscoelasticity has been observed.

In the previous paper, we have investigated the linear viscoelasticity of aqueous solutions of carbohydrates such as sodium alginate[1,2] and methylcellulose[3] using three types of rheometers, which enable us to cover more than 8 decades of frequency range. Entanglement density at various temperatures has also been estimated semiquantitatively by comparing G' and G'' curves and relaxation spectra obtained experimentally with those calculated from the theory of Hayashi.[4] However, the nonlinear viscoelasticity of these aqueous solutions has not been investigated thoroughly. Therefore, in this study the peculiar flow properties of aqueous solution of methylcellulose were compared quantitatively with the recent phenomenological theories of nonlinear viscoelasticity and the experimental results of linear viscoelasticity already reported.[1-3]

Some interesting theories have been proposed for the non-Newtonian viscosity of concentrated polymer solutions. In order to explain the non-Newtonian viscosity of concentrated polymer solutions, Graessley[5,6] has introduced a simplified geometrically constructed entanglement model and assumed a characteristic time for the entanglement formation between molecular chains, which is observed to parallel closely the relaxation time in Rouse theory (τ_R)[7] as given in eq. (1):

$$\tau_R = 6(\eta_0 - \eta_s)M/\pi^2 cRT \tag{1}$$

where η_0 is the zero shear viscosity, η_s is the viscosity of solvent, M is the molecular weight of polymer, c is the concentration of polymer, R is the gas constant, and T is the absolute temperature. However, the entanglement mechanism of the non-Newtonian viscosity is considerably affected by the concentration of polymers, and its quantitative treatment is very difficult, especially in moderately concentrated polymer solutions. Therefore, the relaxation time for the conformational change of an isolated polymer chain[7] seems hardly applicable to the characteristic time for the entanglement formation between polymer chains. Bueche[8] has recognized that the Graessley theory is a significant step foward in the understanding of the nonlinear viscosity effects in fluid polymeric systems, but pointed out that the characteristic time should be an arbitrary constant, and the viscosity master curve in the Graessley theory should not be fixed along the horizontal axis. Williams[9,10] has investigated the viscometric behavior of moderately concentrated polymer solutions by examining the contributions to the stress from the second-order concentration term due to intermolecular force and proposed that the value expressed by eq. (2) should be used for the characteristic time instead of the relaxation time in the Rouse theory:

$$\tau \propto (\eta_0 - \eta_s)/c^2 RT \tag{2}$$

Yamamoto and co-workers[11] have supposed that the entanglement formation time may be of the order of the relaxation time of the breakdown of such an entanglement. It is generally thought that the relaxation spectrum of such a system is distributed over a wide range of relaxation times and the so-called "box"-type region appears. Therefore, they have pointed out that it is reasonable to use the maximum relaxation time in the "box"-type relaxation spectrum for the characteristic time at the zero-shear rate.

As mentioned above, several theories have been proposed for the non-Newtonian viscosity, and the differences among them exist mainly in the evaluation of the characteristic time. Consequently, it is the object of this study to clarify the peculiar flow properties of the aqueous solution of methylcellulose by comparing experimental results with these theories and the experimental results for aqueous solution of sodium alginate which behaves as a polyelectrolyte in solution.

The normal stress effect for solutions of nonpolar polymers has been studied thoroughly by various methods, and a number of phenomenologic theories have been proposed. However, for the aqueous solutions of carbohydrates such as methylcellulose, the normal stress effect has not been

investigated satisfactorily. Particularly, there is no report which deals with this effect from the viewpoint of the relations between the flow properties and the peculiar temperature-dependent intermolecular interactions. Therefore, we constructed a coaxial cylinder apparatus to measure the normal stress in the Couette flow. We measured the extinction angle of the solution by a flow birefringence apparatus to obtain the normal stress difference and investigated the relation between them. The recoverable shear and the non-Hookean behavior in a flow field were also investigated.

EXPERIMENTAL

Measurements

For the measurements of the steady-state shear viscosity in the shear rate range of 10^{-1} to 10^{2} sec^{-1}, a coaxial double-cylinder rheometer was used, in which the outer cup was oscillated or rotated; the inner cylinder was 20 mm in diameter and the outer cup, 22 mm in diameter. Dynamic measurements in the low-frequency range were also made using this rheometer. All measurements were carried out in the methylcellulose concentrations ranging from 0.7% to 3.0% at temperatures of 10°, 25°, and 40°C. The flow birefringence apparatus used was a modified type of that developed by Edsall et al.,[12] which was a coaxial double-cylinder type with the outer cylinder rotating. Detailed descriptions for this apparatus have been given elsewhere.[12] The outer cylinder of the apparatus was 35 mm in diameter and the inner cylinder, 33 mm in diameter. A zirconium arc lamp was used as a light source, and the length of light path in a solution was about 100 mm. The rotational speed was from 30 to 550 rpm, and no turbulence would occur under these conditions. A coaxial cylinder apparatus was constructed to measure the normal stress in Couette flow according to the design of Padden and DeWitt.[13] The outer cylinder of the apparatus was 20 mm in diameter and the inner one, 10 mm in diameter. The inner cylinder was rotated with the same rotational speed as the flow birefringence apparatus.

Sample

The same commercial product of methylcellulose ($\bar{M}_w$ = 110,000) as previously reported[3] was used as sample. To compare the flow properties of aqueous solution of methylcellulose with those of polyelectrolyte solution, sodium alginate (Kamogawa Kagaku Co., $\bar{M}_w$ = 90,000 and 113,000) having narrow molecular weight distribution was used as polyelectrolyte sample. Aqueous solutions of methylcellulose and sodium alginate were prepared by the same procedure as previously reported.[3]

RESULTS AND DISCUSSION

Non-Newtonian Viscosity

A comparison of steady-shear and oscillatory-shear viscosity data is shown in Figure 1, where steady-shear viscosity η, dynamic-shear viscosity

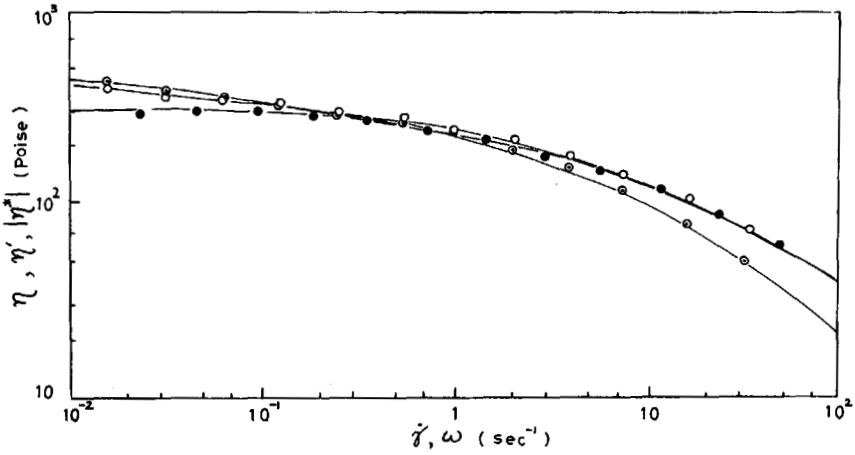

Fig. 1. Logarithmic plots of η, η', and $|\eta^*|$ vs. shear rate $\dot{\gamma}$ or angular frequency ω for an aqueous 3% solution of methylcellulose: (O) absolute value of complex dynamic shear viscosity $|\eta^*|$; (⊙) dynamic shear viscosity η'; (●) steady-shear viscosity η.

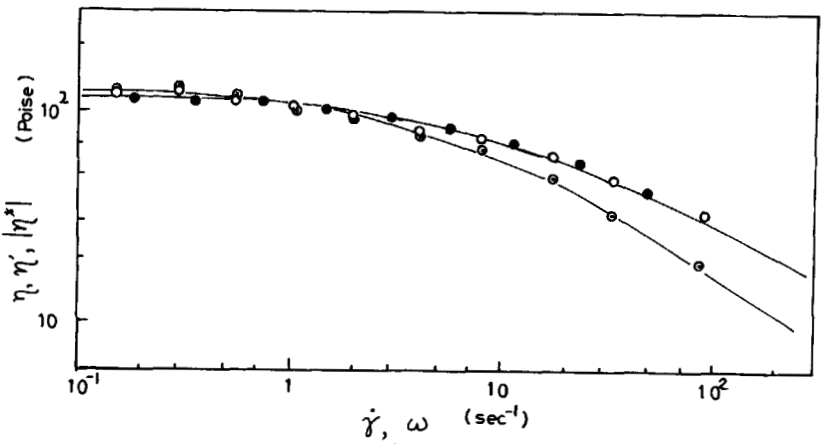

Fig. 2. Logarithmic plots of η, η', and $|\eta^*|$ vs. shear rate $\dot{\gamma}$ or angular frequency ω for an aqueous 3% solution of sodium alginate: (O) absolute value of complex dynamic shear viscosity $|\eta^*|$; (⊙) dynamic shear viscosity η'; (●) steady-shear viscosity η.

η', and the absolute value of the complex viscosity $|\eta^*|$ obtained by using the coaxial doublecylinder rheometer are given as a function of shear rate $\dot{\gamma}$ or angular frequency ω for an aqueous 3% solution of methylcellulose. The absolute value of the complex viscosity may be expressed as

$$|\eta^*| = [(\eta')^2 + (G'/\omega)^2]^{1/2} \tag{3}$$

where G' is the storage modulus. The results for an aqueous 3% solution of sodium alginate having $\bar{M}_w$ of 90,000 are shown in Figure 2. As the molecular weight of methylcellulose is larger than that of sodium alginate, the zero-shear viscosity η_0 for the aqueous solution of methylcellulose is

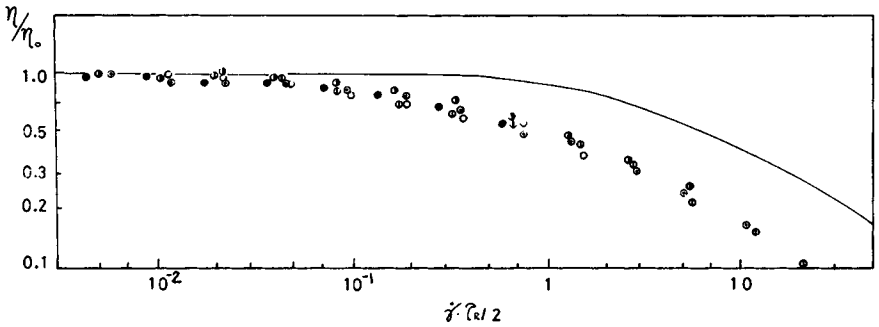

Fig. 3. Ratio of steady shear viscosity to initial viscosity η/η_0 vs. reduced shear rate $\dot{\gamma}\tau_R/2$ for aqueous solutions of methylcellulose at 10°C. Concentration: (⊕) 3%; (⊙) 2%; (◑) 1.5%; (○) 1%; (●) 0.7%.

higher than that for the aqueous solution of sodium alginate. Excellent agreement between η and $|\eta^*|$ has been observed by Mendelson et al.,[14] for polyethylene melt over the region of overlapping data, and η' diverges from the $|\eta^*|$ curve in the region where η becomes non-Newtonian. In the present study, the results for the aqueous solution of sodium alginate given in Figure 2 show the same tendency as the results of Mendelson. However, for the aqueous solution of methylcellulose, the values of $|\eta^*|$ agree with those of η at the high-shear rate range, but at the low-shear rate range the values of $|\eta^*|$ and η' are larger than those of η, and the dynamic data depend slightly on the frequency. It is thought that the phenomena observed for the aqueous solution of methylcellulose are attributed to the peculiar entanglement mechanism and also to the broad molecular weight distribution of methylcellulose as indicated by Adams[15] for molten polypropylene. The non-Newtonian behavior in the aqueous solution of sodium alginate is observed to occur at the same shear rate region as in the aqueous solution of methylcellulose, even though the molecular weight of sodium alginate is smaller than that of methylcellulose. These phenomena seem to be attributed to the extended configuration of polyelectrolyte in solution, resulting in intermolecular interactions even in very dilute concentrations.

Since Graessley has developed the theory of non-Newtonian viscosity,[5,6] many investigations on the non-Newtonian viscosity of polymer solutions have been carried out phenomenologically and theoretically in relation to his theory. The plots of η/η_0 as a function of the reduced shear rate $\tau\dot{\gamma}/2$ for the aqueous solutions of methylcellulose in concentrations ranging from 0.7 % to 3% at 10°, 25°, and 40°C are shown in Figures 3, 4, and 5, respectively, where Rouse's relaxation time[7] is adopted for the characteristic time τ as in the Graessley theory.[5,6] The solid lines were calculated from the Graessley theory considering the polydispersity of the sample. These results indicate that the significant discrepancies, which appears to be more than experimental error, exist between the experimental data and the theoretical curves in these figures. The non-Newtonian behavior is observed to occur at the lower reduced shear rate than the theoretical

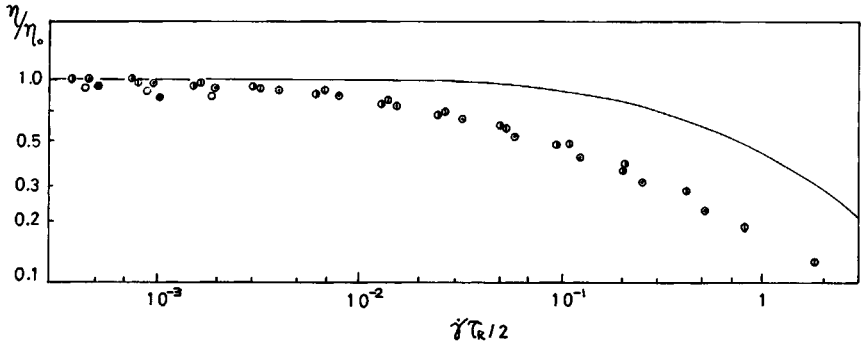

Fig. 4. Ratio of steady-shear viscosity to initial viscosity η/η_0 vs. reduced shear rate $\dot{\gamma}\tau_R/2$ for aqueous solutions of methylcellulose at 25°C. Concentration: (⊙) 3%; (⊙) 2%; (◑) 1.5%; (○) 1%; (●) 0.7%.

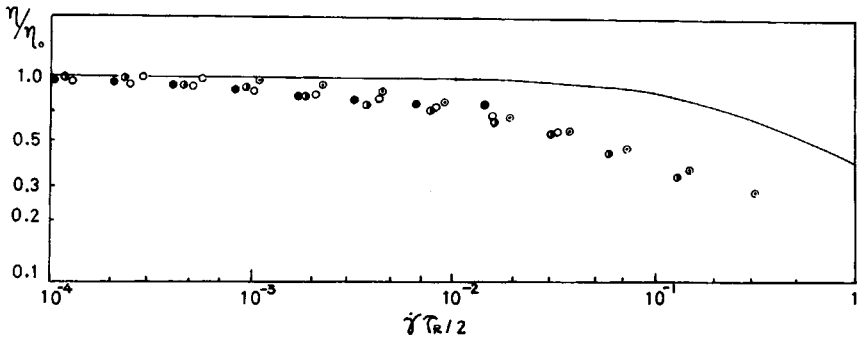

Fig. 5. Ratio of steady-shear viscosity to initial viscosity η/η_0 vs. reduced shear rate $\dot{\gamma}\tau_R/2$ for aqueous solutions of methylcellulose at 40°C. Concentration: (⊙) 2%; (◑) 1.5%; (○) 1%, (●) 0.7%.

curves. When the theories of the non-Newtonian viscosity are applied to experimental data, the major problem is the evaluation of the characteristic time for the entanglement formation as mentioned above. This is the reason why many theories of non-Newtonian viscosity are proposed. By comparing the relaxation spectra obtained experimentally with the theoretical spectra calculated from the Hayashi theory,[4] we have succeeded in the evaluation of the maximum relaxation time τ_{max} in the "box"-type relaxation spectrum for the aqueous solution of methylcellulose.[3] Then we examined the adaptability of τ_{max} to the characteristic time from the same viewpoint as Yamamoto et al.[11] had presented.

Table I shows the characteristic times at various concentrations and temperatures for the aqueous solutions of methylcellulose, where τ_R indicates the maximum relaxation time in the Rouse theory.[7] The experimental characteristic time τ_0 was obtained by shifting the plots of η/η_0 versus $\tau_R\dot{\gamma}/2$ along the abscissa until all coincide on the theoretical curve. The X/q term indicates the entanglement density in the Hayashi theory[4] and was used for the calculation of τ_{max}. Table I also includes the values of

TABLE I
Characteristic Times

Sample	Temp., °C	Concentration, wt-%	$\tau_R \times 10^2$, sec	$\tau_0 \times 10^2$, sec	$\tau_{max} \times 10^2$, sec	τ_0/τ_R	X/q
Methylcellulose	10	1.0	0.171	1.55	3.75	9.08	2.8
		1.5	0.569	4.06	15.4	7.14	3.0
		2.0	1.37	8.64	58.6	6.33	3.5
		3.0	4.65	25.1	235.0	5.40	3.7
	25	1.0	0.0732	0.472	1.29	6.45	2.6
		1.5	0.216	1.29	4.74	5.95	2.8
		2.0	0.540	2.95	16.1	5.46	3.1
		3.0	1.850	9.23	209.0	5.00	3.7
	40	1.0	0.0348	0.552	0.544	10.5	2.5
		1.5	0.137	1.49	4.09	9.50	3.1
		2.0	0.309	2.16	14.4	6.99	3.6
Sodium alginate	25	2.0	0.297	7.82	7.28	26.2	3.0
		3.0	0.808	22.2	21.8	27.5	3.0
		5.0	3.04	36.3	99.1	11.9	3.0

τ_R, τ_0, and τ_{max} for the aqueous solutions of sodium alginate at 25°C. The deviation of experimental results from the Graessley theory is indicated by τ_0/τ_R. The values of τ_{max} agree relatively well with those of τ_0 for the aqueous solution of sodium alginate, but for the aqueous solution of methylcellulose the values of τ_{max} are larger than those of τ_0. The experimental results mentioned above for the aqueous solution of methylcellulose are thought to be related to the difference between the value of $|\eta^*|$ corresponding to the linear viscoelasticity and that of η corresponding to the non-linear viscoelasticity at a large deformation at low frequency and low-shear rate regions as observed in Figure 1. With increasing polymer concentration, the difference between τ_0 and τ_{max} increases, but that between τ_0 and τ_R decreases.

The latter tendency can be explained by the modified Graessley theory.[16] Then the applicability of τ_{max} to the characteristic time for the entanglement formation is doubtful in an intermediate concentration range. For the aqueous solution of methylcellulose, the temperature dependence of τ_0/τ_R is not definite. For the aqueous solution of sodium alginate, the value of τ_0/τ_R is extremely larger than that for the aqueous solution of methylcellulose. This tendency corresponds to the results shown in Figure 2, in which the steady-state viscosity for the aqueous solution of sodium alginate becomes non-Newtonian at the same shear rate range even though molecular weight is low.

These phenomena depend on the characteristics of polyelectrolytic solutions such as an extended configuration and a peculiar entanglement mechanism, and these peculiarities are shown clearly by the concentration dependence of the zero-shear viscosity η_0. The relation between the concentration dependence of η_0 and the configuration of molecular chains for

the aqueous solution of sodium alginate has been reported in the previous papers.[1,3] For the aqueous solution of methylcellulose, the values of η_0 were proportional to the 4.4th power of concentrations at 25°C, and the concentration dependence of η_0 increased with increasing temperature. Therefore, it is thought that the structural networks in solution become closer with increasing temperature. For the aqueous solution of sodium alginate, the values of η_0 were proportional to the 3.8th power of the concentrations. These results indicate the extremely extended configuration of molecular chains of sodium alginate. However, the concentration dependence of η_0 increased with the addition of NaCl as a result of depression of the electrostatic repulsion between molecular chains.

Normal Stress Effect

The normal stress difference was calculated according to the procedure by Coleman and Noll[17] and Markovitz.[18,19] In the present study, the rate of shear function $\lambda(S)$ was calculated initially from the steady-state viscosity according to the differentiation method of Krieger.[20] The thrust difference ΔP between the inner and outer cylinders is related to the normal stress functions $\hat{\sigma}_1(S)$ and $\hat{\sigma}_2(S)$ by the following equation:

$$\Delta P = \int_{R_1}^{R_2} \frac{1}{r} [\hat{\sigma}_2(S_r) - \hat{\sigma}_1(S_r)]dr - \int_{R_1}^{R_2} \rho r[\omega(r)]dr \tag{4}$$

$$S_r = M_T/2\pi r^2 \tag{5}$$

where ρ is the density; $\omega(r)$ and S_r are the angular velocity and the shear stress of a particle of fluid at a distance r from the axis, respectively; and M_T is the torque per unit height applied to the turning cylinder. The relation between the angular velocity Ω and the shear stress S_1 at the turning cylinder is given by eq. (6):

$$\Omega = \frac{1}{2} \int_{S_2}^{S_1} \lambda(S)/S \cdot dS \tag{6}$$

where S_2 is the shear stress at the outer cylinder. S_2 is related to S_1 by the following equation:

$$S_2 = S_1(R_1/R_2)^2 \tag{7}$$

where R_1 and R_2 are the radii of the inner and outer cylinder, respectively. The function of $\Omega(S_1)$ can be computed according to eq. (6) by suitable numerical integration, and then the graph of $\Omega(S_1)$ can be used to read off values of S_1 corresponding to the speed of rotation. The normal stress difference at the inner cylinder $\hat{\sigma}_2(S_1) - \hat{\sigma}_1(S_1)$ is then obtained by the following procedure: A corrected thrust difference ΔP_c is defined by

$$\Delta P_c = \Delta P + \int_{R_1}^{R_2} \rho r[\omega(r)]^2 dr. \tag{8}$$

The function $\Psi(S)$ is defined by

$$\Psi(S_1) = 2S_1 \cdot d\Delta P_c/dS_1. \tag{9}$$

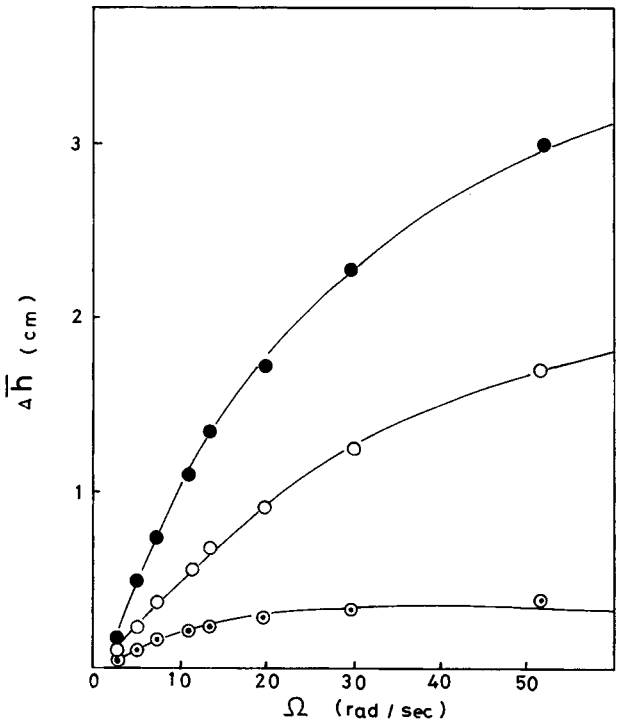

Fig. 6. Pressure rise in a coaxial cylinder apparatus as a function of rotational speed of the inner cylinder for aqueous solutions of methylcellulose at 25°C. Concentration: (●) 3%; (○) 2.5%; (◐) 2%.

Then the value of $\hat{\sigma}_2(S_1) - \hat{\sigma}_1(S_1)$ is calculated by solving eq. (10):

$$\hat{\sigma}_2(S_1) - \hat{\sigma}_1(S_1) = \sum_{n=0}^{\infty} \Psi[(R_1/R_2)^{2n} \cdot S_1]. \tag{10}$$

In Figure 6, the pressure rise $\Delta\bar{h}$ in the inner cylinder of the coaxial cylinder apparatus averaged over the values obtained in the two senses of rotation is plotted against the angular velocity of the inner cylinder for the aqueous solution of methylcellulose in concentrations ranging from 2% to 3% at 25°C. The $\Delta\bar{h}$ values increased rapidly in the range of low angular velocities, but approached an equilibrium value with increasing angular velocity. For the same solution, the relation between shear rate $\dot{\gamma}$ and shear stress S_1 at the inner cylinder is shown in Figure 7. From these results, ΔP_c and $\Psi(S_1)$ were calculated from eqs. (8) and (9), and then the normal stress difference $\hat{\sigma}_2(S_1) - \hat{\sigma}_1(S_1)$ was obtained. Figure 8 shows ΔP_c, $\Psi(S_1)$, and $\hat{\sigma}_2(S_1) - \hat{\sigma}_1(S_1)$ plotted against S_1 for a 2.5% aqueous solution of methylcellulose at 25°C. The relations between $\hat{\sigma}_2(S_1) - \hat{\sigma}_1(S_1)$ and S_1 for the aqueous solution of methylcellulose in the concentrations ranging from 1.5% to 2.5% at various temperatures are shown in Figure 9. The results for the aqueous solution of sodium alginate in

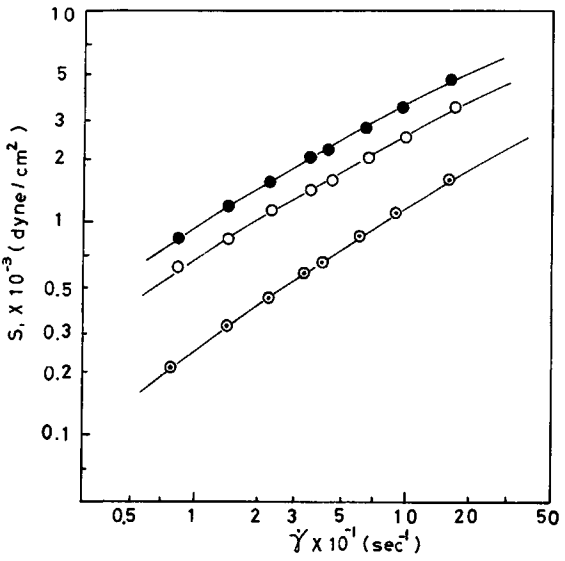

Fig. 7. Logarithmic plots of S_1 vs. $\dot{\gamma}$ for aqueous solutions of methylcellulose at 25°C. Concentration: (●) 3%; (○) 2.5%; (⊙) 2%.

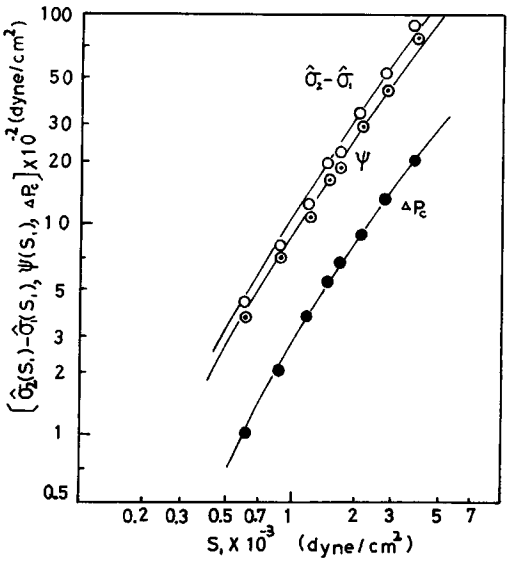

Fig. 8. Logarithmic plots of ΔP_c, ψ, and $\hat{\sigma}_2(S_1) - \hat{\sigma}_1(S_1)$ vs. S_1 for aqueous 2.5% solution of methylcellulose at 25°C.

concentrations ranging from 3% to 5% at 25°C are also plotted in Figure 9. The results for the aqueous solution of methylcellulose are represented approximately by a single curve irrespective of temperature and concentration, and this is the same tendency as the results for a solution of polyisobutyrene in cetane.[19] Both results are numerically similar to each other.

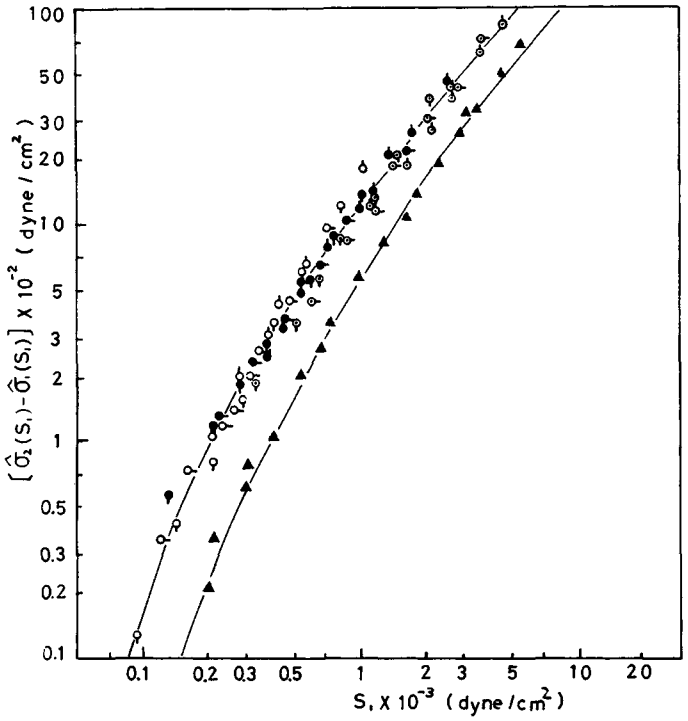

Fig. 9. Logarithmic plots of $\hat{\sigma}_2(S_1) - \hat{\sigma}_1(S_1)$ vs. S_1 for aqueous solutions of methylcellulose and sodium alginate. Methylcellulose: (♁) 1.5%, 10°C; (●) 2.0%, 10°C; (⊙) 2.5%, 10°C; (○-) 1.5%, 25°C; (●-) 2.0%, 25°C; (⊙-) 2.5%, 25°C; (♀) 1.5%, 40°C; (●) 2.0%, 40°C; (♀) 2.5%, 40°C. Sodium alginate: (▲).

However, the results for the aqueous solution of sodium alginate as polyelectrolyte solution lie below the curve for the aqueous solution of methylcellulose.

The relations between extinction angle χ and $\dot{\gamma}$ for the 1% and 2% aqueous solutions of methylcellulose at various temperatures are shown in Figure 10. In the range of lower shear rates, the values of χ decrease rapidly, but approach an equilibrium value with increasing shear rate. The relation between the loss angle and the angular frequency in linear viscoelastic measurements also shows the same tendency, but the correlation between the loss angle and χ is not obvious. The values of χ become larger with increasing temperature and decreasing concentration. It is well known that the normal stress difference can be calculated from χ and shear stress S_1 according to eq. (11):

$$\hat{\sigma}_2(S_1) - \hat{\sigma}_1(S_1) = 2S_1\cot 2\chi. \tag{11}$$

The normal stress differences obtained with the Couette-type apparatus and those calculated from χ according to eq. (11) are shown in Figures 11 and 12 for the 1.5% and 2% aqueous solutions of methylcellulose at various temperatures. From these results, the values of normal stress

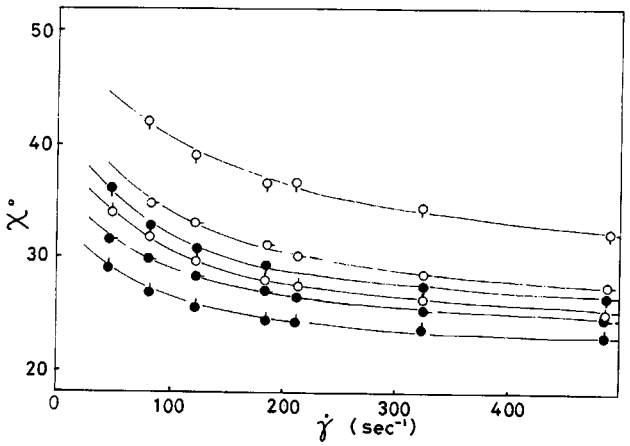

Fig. 10. Plots of χ vs. $\dot{\gamma}$ for aqueous 1% and 2% solutions of methylcellulose. 1% Solution: (δ) 10°C; (o-) 25°C; (♀) 40°C. 2% Solution: (●) 10°C; (●-) 25°C; (●) 40°C.

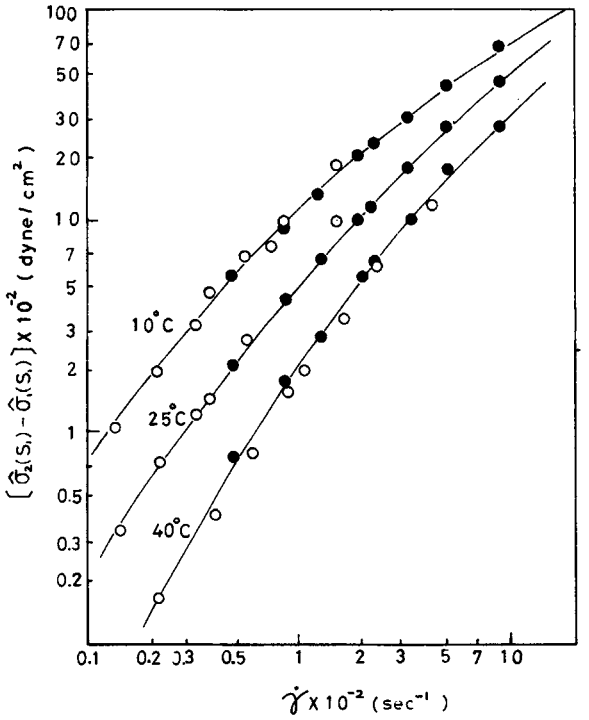

Fig. 11. Logarithmic plots of $\hat{\sigma}_2(S) - \hat{\sigma}_1(S_1)$ vs. $\dot{\gamma}$ for aqueous 1.5% solution of methylcellulose at various temperatures: (O) obtained from normal thrust; (●) obtained from flow birefringence.

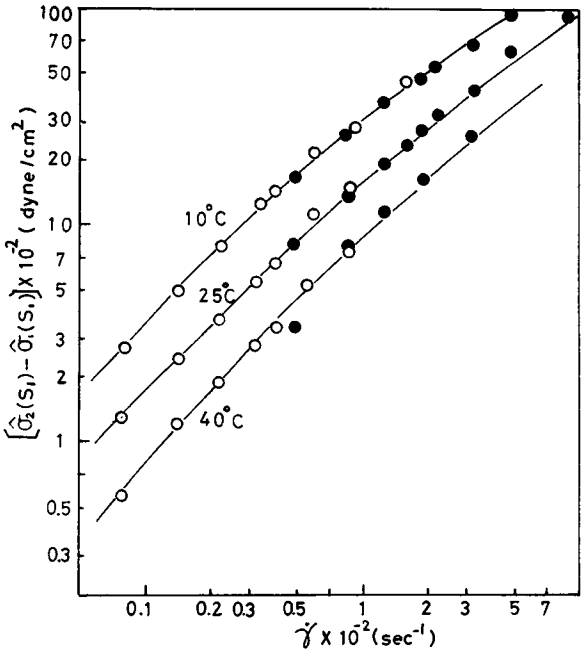

Fig. 12. Logarithmic plots of $\hat{\sigma}_2(S_1) - \hat{\sigma}_1(S_1)$ vs. $\dot{\gamma}$ for aqueous 2.0% solution of methylcellulose at various temperatures: (O) obtained from normal thrust; (●) obtained from flow birefringence.

differences determined by the optical and mechanical methods coincided with each other. Therefore, it is thought that the coaxiality of the stress and polarizability tensors is proved for the aqueous solution of methylcellulose, whose backbone consists of pyranose rings, as reported for solutions of nonpolar polymers in this shear rate range.

Recoverable Shear

The relation among normal stress, shear stress, extinction angle, and recoverable shear s may be written as follow:

$$s = [\hat{\sigma}_2(S_1) - \hat{\sigma}_1(S_1)]/S_1 = 2 \cot 2\chi \tag{12}$$

Figure 13 shows the values of s plotted against $\dot{\gamma}$ for the aqueous solution of methylcellulose in concentrations ranging from 1.5% to 2.5% at various temperatures. With increasing concentration, the $\dot{\gamma}$ dependence of s decreases and the temperature dependence of s becomes smaller. It is thought that the structural networks in a solution become closer with increasing concentration and temperature, and as it is difficult for the molecular chains in solution to extent to the direction of shear, an upper limit of s exists. The relations between s and S_1 for an aqueous solution of methylcellulose in concentrations ranging from 0.7% to 2.5% at various temperatures are logarithmically plotted in Figures 14, 15, and 16; and those for aqueous solutions of sodium alginate with the same order of mo-

lecular weight as methylcellulose in concentrations ranging from 3% to 5% at 25°C are shown in Figure 17. The slopes m of the linear portion of the log s-versus log S_1-plots are given in Table II for the aqueous solution of methylcellulose. The temperature dependence of m is remarkable in

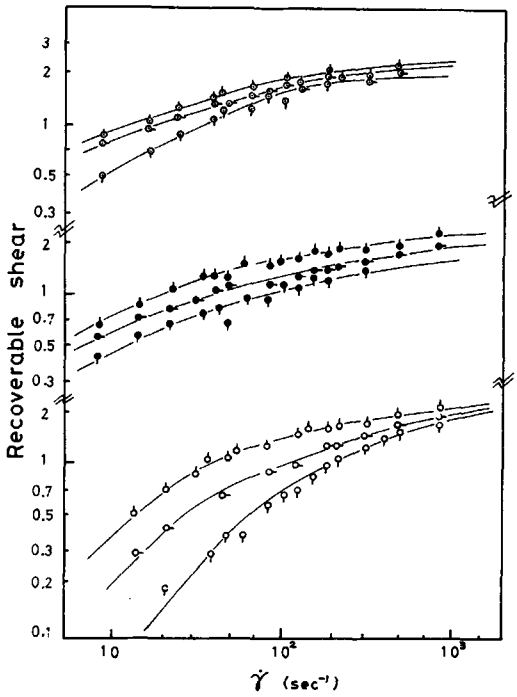

Fig. 13. Logarithmic plots of s vs. $\dot{\gamma}$ for aqueous solutions of methylcellulose: (♁) 1.5%, 10°C; (○-) 1.5%, 25°C; (♀) 1.5%, 40°C; (◐) 2.0%, 10°C; (●-) 2.0%, 25°C; (◐) 2.0%, 40°C; (♁) 2.5%, 10°C; (⊙-) 2.5%, 25°C; (♀) 2.5%, 40°C.

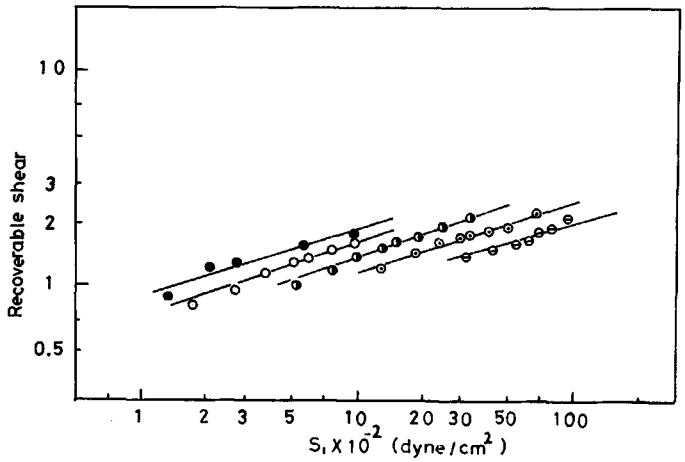

Fig. 14. Logarithmic plots of s vs. S_1 for aqueous solutions of methylcellulose at 10°C. Concentration: (⊖) 2.5%; (⊙) 2.0%; (◑) 1.5%; (○) 1.0%; (●) 0.7%.

dilute solutions and becomes smaller with increasing concentration. At higher temperature, the values of m and their concentration dependence are larger. On the other hand, the values of m for the aqueous solution of sodium alginate are 0.65 at 2%, 0.60 at 3%, and 0.65 at 5%, respectively.

TABLE II
Values of m for Aqueous Solutions of Methylcellulose

	Concentration, wt-%				
Temp., °C	0.7	1.0	1.5	2.0	2.5
10	0.36	0.33	0.33	0.31	0.30
25	0.60	0.50	0.50	0.45	0.35
40	1.05	0.75	0.73	0.55	—

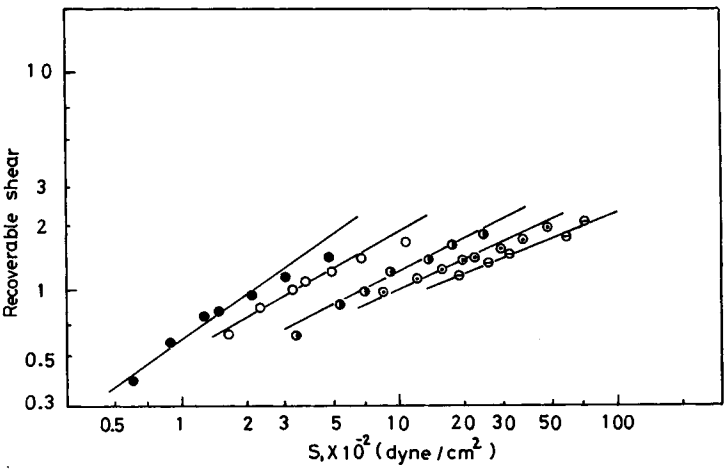

Fig. 15. Logarithmic plots of s vs. S_1 for aqueous solutions of methylcellulose at 25°C. Concentration: (⊖) 2.5%; (⊙) 2.0%; (◐) 1.5%; (○) 1.0%; (●) 0.7%.

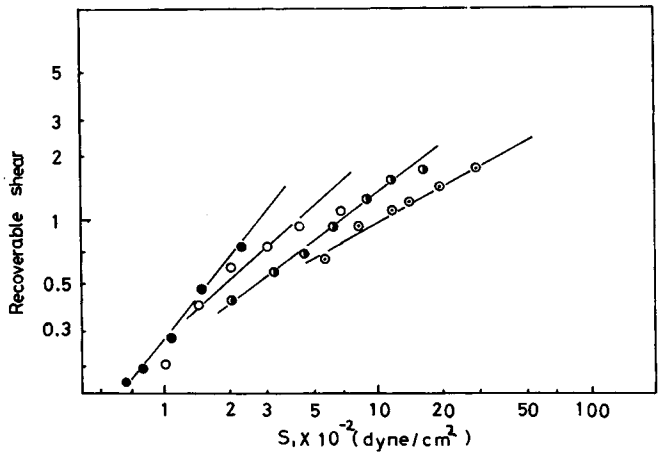

Fig. 16. Logarithmic plots of s vs. S_1 for aqueous solutions of methylcellulose at 40°C. Concentration: (⊙) 2.0%; (◑) 1.5%; (○) 1.0%; (●) 0.7%.

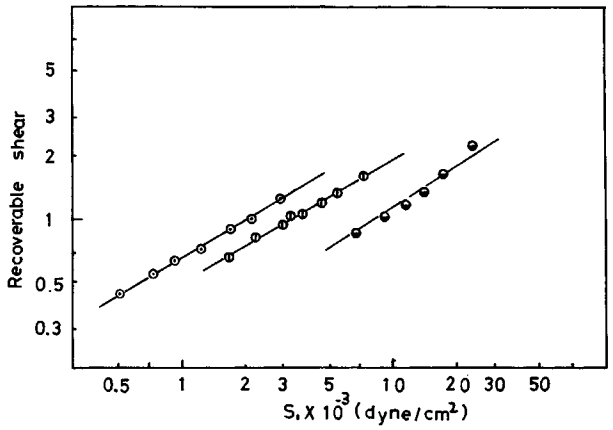

Fig. 17. Logarithmic plots of s vs. S_1 for aqueous solutions of sodium alginate at 25°C. Concentration: (◒) 5.0%; (◑) 3.0%; (⊙) 2.0%.

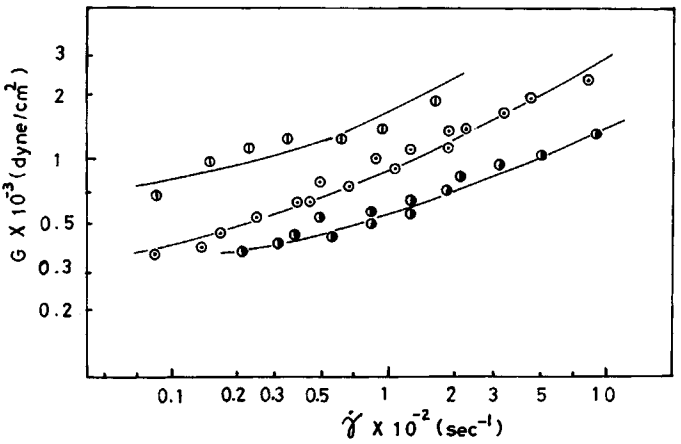

Fig. 18. Logarithmic plots of G vs. $\dot{\gamma}$ for aqueous solutions of methylcellulose at 25°C. Concentration: (◑) 3.0%; (⊙) 2.0%; (◑) 1.5%.

Namely, for the aqueous solution of sodium alginate the concentration dependence of m is not definite, and this fact indicates that the effect of concentration on the intermolecular interactions for a polyelectrolyte solution is not so strong as that for a nonpolyelectrolyte solution and coincides with the tendency of the concentration dependence of η_0.

From $m = 1$, "Hooke's law in shear" holds, and this has been proved experimentally by Philippoff[21] and Kotaka et al.[22] For the aqueous solution of methylcellulose, the values of m, except that for a concentration of 0.7% and at 40°C, were smaller than 1.0. It is thought that the phenomena observed for the aqueous solution of methylcellulose are attributed to the strong intermolecular interactions and the relatively high stiffness of cellulose chains as pointed out by Kotaka et al.,[22] especially the stretching-out effect of polymer chains becomes significant and characterizes the

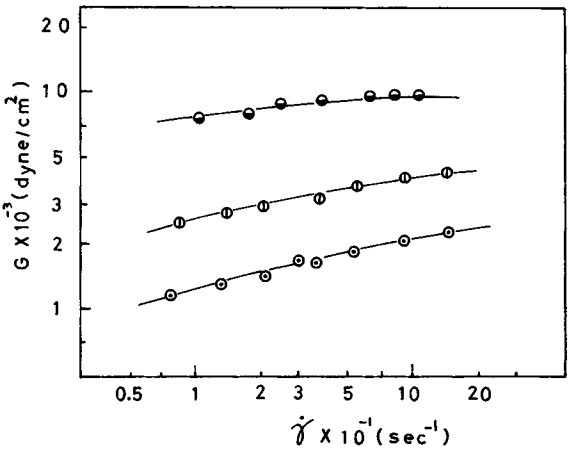

Fig. 19. Logarithmic plots of G vs. $\dot{\gamma}$ for aqueous solutions of sodium alginate at 25°C. Concentration: (●) 5.0%; (①) 3.0%; (⊙) 2.0%.

flow properties for the aqueous solution of methylcellulose. As the stretching-out effect depends on the imperfection of the structural networks as well as the extension of the molecular chains, the effect is extremely remarkable for the aqueous solution of methylcellulose, in which the molecular weight distribution is broad and the network structure is formed by geometric entanglements and secondary bonding such as hydrogen bonds.

In Figures 18 and 19, the fluid elasticity G defined by eq. (13),

$$G = S_1/s = S_1/(2 \cot 2\chi) \tag{13}$$

is plotted against $\dot{\gamma}$ for aqueous solutions of methylcellulose and sodium alginate. The shear rate dependence of G is shown in Figures 18 and 19. The shear rate dependence of G for the aqueous solution of methylcellulose is more remarkable than that for the aqueous solution of sodium alginate. The remarkable shear rate dependence of G for the aqueous solution of methylcellulose is assumed to depend on the non-Hookean behavior of elastic mechanism. The G values for the aqueous solution of sodium alginate are higher than those for the aqueous solution of methylcellulose at the same shear rate. That tendency can be explained by the peculiarity of polyelectrolytic polymers such as the extended configuration and the remarkable orientation entoropy as pointed out by Kuroiwa and Nakamura.[23]

The authors wish to thank Dr. S. Nakamura for his useful suggestions.

References

1. T. Amari and M. Nakamura, *Kogyo Kagaku Zasshi* (*J. Chem. Soc. Japan, Ind. Chem. Sect.*), **74**, 2140 (1971).
2. M. Nakamura and T. Amari, *J. Soc. Mater. Sci. Japan*, **20**, 638 (1971).
3. T. Amari and M. Nakamura, *J. Appl. Polym. Sci.*, **17**, 589 (1973).
4. S. Hayashi, *J. Phys. Soc. Japan*, **19**, 2306 (1964).

5. W. W. Graessley, *J. Chem. Phys.*, **43**, 2969 (1965).
6. W. W. Graessley, *ibid.*, **47**, 1942 (1967).
7. P. E. Rouse, *ibid.*, **21**, 1272 (1953).
8. F. Bueche, *ibid.*, **48**, 4781 (1968).
9. M. C. Williams, *A.I.Ch.E. J.*, **13**, 534 (1967).
10. M. C. Williams, *ibid.*, **14**, 360 (1968).
11. T. Tanaka, M. Yamamoto, and Y. Takano, *J. Macromol. Sci.-Phys.*, **B4**, 931 (1970).
12. J. T. Edsall, A. Rich, and M. Goldstein, *Rev. Sci. Inst.*, **23**, 695 (1952).
13. F. J. Padden and T. W. DeWitt, *J. Appl. Phys.*, **25**, 1086 (1954).
14. R. A. Mendelson, W. A. Bowles, and F. L. Finger, *J. Polym. Sci. A-2*, **8**, 105 (1970).
15. J. W. Adams, H. Janeschitz-Kriegl, J. L. DenOtter, and J. L. S. Wales, *J. Polym. Sci. A-2*, **6**, 871 (1968).
16. W. W. Graessley and L. Segal, *Macromolecules*, **2**, 49 (1969).
17. B. D. Coleman and W. Noll, *Arch. Rotional Mech. Anal.*, **3**, 289 (1959).
18. H. Markovitz, *Trans. Soc. Rheol.*, **1**, 37 (1957).
19. H. Markovitz, in *Rheology*, Vol. 4, E. R. Eirich, Ed., Academic Press, New York, 1967, p. 347.
20. I. M. Krieger and H. Elrod, *J. Appl. Phys.*, **25**, 1086 (1954).
21. W. Philippoff, *J. Appl. Phys.*, **27**, 984 (1956).
22. T. Kotaka, M. Kurata, and M. Tamura, *ibid.*, **30**, 1705 (1959).
23. S. Kuroiwa and M. Nakamura, *Kobunshi Kagaku* (*Chem. High Polym.*), **22**, 394 (1965).

Received December 6, 1972
Revised April 23, 1973